Articles

A Mechanistic Study of the Reaction between a Diiron(II) Complex $[Fe^{II}_2(\mu\text{-}OH)_2(6\text{-}Me_3\text{-}TPA)_2]^{2+}$ and O_2 to Form a Diiron(III) Peroxo Complex

Sergey V. Kryatov and Elena V. Rybak-Akimova*

Department of Chemistry, Tufts University, Medford, Massachusetts 02155

Vicki L. MacMurdo and Lawrence Que, Jr.*

Department of Chemistry and Center for Metals in Biocatalysis, University of Minnesota, Minneapolis, Minnesota 55455

Received November 17, 2000

A kinetic study of the reaction between a diiron(II) complex $[Fe^{II}_2(\mu\text{-}OH)_2(6\text{-}Me_3\text{-}TPA)_2]^{2+}$ **1**, where 6-Me_3-TPA = tris(6-methyl-2-pyridylmethyl)amine, and dioxygen is presented. A diiron(III) peroxo complex $[Fe^{III}_2(\mu\text{-}O)(\mu\text{-}O_2)(6\text{-}Me_3\text{-}TPA)_2]^{2+}$ **2** forms quantitatively in dichloromethane at temperatures from −80 to −40 °C. The reaction is first order in $[Fe^{II}_2]$ and $[O_2]$, with the activation parameters $\Delta H^{\ddagger} = 17 \pm 2$ kJ mol^{-1} and $\Delta S^{\ddagger} = -175 \pm 20$ J mol^{-1} K^{-1}. The reaction rate is not significantly influenced by the addition of H_2O or D_2O. The reaction proceeds faster in more polar solvents (acetone and acetonitrile), but the yield of **2** is not quantitative in these solvents. Complex **1** reacts with NO at a rate about 10^3 faster than with O_2. The mechanistic analysis suggests an associative rate-limiting step for the oxygenation of **1**, similar to that for stearoyl-ACP Δ^9-desaturase, but distinct from the probable dissociative pathway of methane monoxygenase. An η^1-superoxo $Fe^{II}Fe^{III}$ species is a likely steady-state intermediate during the oxygenation of complex **1**.

Introduction

A number of proteins utilize non-heme diiron centers to bind or activate dioxygen. There are many similarities among these proteins, including a common reaction between the reduced diiron(II) form and O_2 to yield a diiron(III) peroxo adduct.[1−5] For the invertebrate oxygen carrier hemerythrin, this process is reversible.[6−11] However for several others (soluble methane monooxygenase,[12,13] stearoyl-ACP Δ^9-desaturase,[14] and ferritin[15]) a diiron(III) peroxo species is the first intermediate to be detected on the metabolic pathway for dioxygen utilization. Class I ribonucleotide reductase (RNR), common to animals, plants, and many simpler organisms, has non-heme diiron centers in its R2 subunit, which participate in the generation of a tyrosyl radical required as a catalyst for the reduction of ribonucleotides to deoxyribonucleotides.[16] The R2 RNR protein from *Escherichia coli* has been thoroughly studied and is currently believed to function through $Fe^{II}Fe^{II}$, $Fe^{III}Fe^{III}$-peroxo, $Fe^{III}Fe^{IV}$, and $Fe^{III}Fe^{III}$-oxo states (Scheme 1).[1,17−21] The formation of a diiron(III) peroxo intermediate, while tentative for the native R2 RNR,[22] has been firmly established for the D84E mutant.[18,19]

The biochemical importance of the diiron(II) unit oxygenation to diiron(III) peroxo species has stimulated investigations at the

* Corresponding author.

(1) Solomon, E. I.; Brunold, T. C.; Davis, M. I.; Kemsley, J. N.; Lee, S.-K.; Lehnert, N.; Neese, F.; Skulan, A. J.; Yang, Y.-S.; Zhou, J. *Chem. Rev.* **2000**, *100*, 235−349.
(2) Du Bois, J.; Mizoguchi, T. J.; Lippard, S. J. *Coord. Chem. Rev.* **2000**, *200*−*202*, 443−485.
(3) Kurtz, D. M., Jr. *J. Inorg. Biol. Chem.* **1997**, *2*, 159−167.
(4) Wallar, B. J.; Lipscomb, J. D. *Chem. Rev.* **1996**, *96*, 2625−2657.
(5) Feig, A. L.; Lippard, S. J. *Chem. Rev.* **1994**, *94*, 759−805.
(6) Brunold, T. C.; Solomon, E. I. *J. Am. Chem. Soc.* **1999**, *121*, 8288−8295.
(7) Lloyd, C. R.; Eyring, E. M.; Ellis, W. R., Jr. *J. Am. Chem. Soc.* **1995**, *117*, 11993−11994.
(8) Howard, J. B.; Rees, D. C. *Adv. Protein Chem.* **1991**, *42*, 199−280.
(9) Wilkins, P. C.; Wilkins, R. G. *Coord. Chem. Rev.* **1987**, *79*, 195−214.
(10) Wilkins, R. G. In *Kinetics of Formation of Biological Oxygen Carriers*; Wilkins, R. G., Ed.; Plenum Press: New York, 1987; pp 49−60.
(11) Petrou, A. L.; Armstrong, F. A.; Sykes, A. G.; Harrington, P. C.; Wilkins, R. G. *Biochim. Biophys. Acta* **1981**, *670*, 377−384.
(12) Lee, S.-K.; Lipscomb, J. D. *Biochemistry* **1999**, *38*, 4423−4432.
(13) Valentine, A. M.; Stahl, S. S.; Lippard, S. J. *J. Am. Chem. Soc.* **1999**, *121*, 3876−3887.
(14) Broadwater, J. A.; Achim, C.; Münck, E.; Fox, B. G. *Biochemistry* **1999**, *38*, 12197−12204.
(15) Hwang, J.; Krebs, C.; Huynh, B. H.; Edmondson, D. E.; Theil, E. C.; Penner-Hahn, J. E. *Science* **2000**, *287*, 122−125.
(16) Voet, D.; Voet, J. *Biochemistry*; Wiley: New York, 1995.
(17) Stubbe, J.; Riggs-Gelasco, P. *Trends Biochem. Sci.* **1998**, *23*, 438−443.
(18) Bollinger, J. M., Jr.; Krebs, C.; Vicol, A.; Chen, S. X.; Ley, B. A.; Edmondson, D. E.; Huynh, B. H. *J. Am. Chem. Soc.* **1998**, *120*, 1094−1095.
(19) Voegtli, W. C.; Khidekel, N.; Baldwin, J.; Ley, B. A.; Bollinger, J. M., Jr.; Rosenzweig, A. C. *J. Am. Chem. Soc.* **2000**, *122*, 3255−3261.
(20) Andersson, M. E.; Höegbom, M.; Rinaldo-Matthis, A.; Andersson, K. K.; Sjöeberg, B.-M.; Nordlund, P. *J. Am. Chem. Soc.* **1999**, *121*, 2346−2352.
(21) Yang, Y.-S.; Baldwin, J.; Ley, B. A.; Bollinger, J. M., Jr.; Solomon, E. I. *J. Am. Chem. Soc.* **2000**, *122*, 8495−8510.
(22) Tong, W. H.; Chen, S.; Lloyd, S. G.; Edmondson, D. E.; Huynh, B. H.; Stubbe, J. *J. Am. Chem. Soc.* **1996**, *118*, 2107−2108.

10.1021/ic001300k CCC: $20.00
Published on Web 04/06/2001

Scheme 1

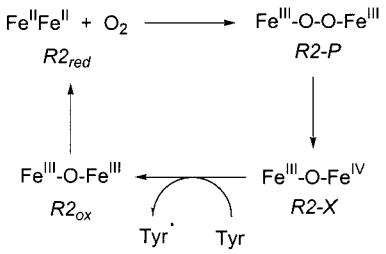

level of synthetic inorganic model complexes during the past decade.[2,23] Oxygenation of synthetic non-heme diiron(II) complexes with adjacent Fe^{II} ions usually gives oxo-bridged diiron(III) species as final products, but diiron(III) peroxo adducts can be often observed as intermediates and sometimes can even be isolated and characterized.[2,23−28] The known diiron(III) peroxo complexes are all unstable thermodynamically and can form quantitatively only when the rate of their formation is much higher than the rate of their decomposition.[25,26] A limited number of such reactions of a diiron(II) complex with O_2 to form a diiron(III) peroxo species have been studied in detail using kinetic techniques.[24,27] The results complement the analogous kinetic investigations of the native diiron(II) proteins.[7,10−14]

An alternative synthetic route to the diiron(III) peroxo species is the reaction between diiron(III) hydroxo- or oxo-precursors with H_2O_2.[23,29−31] In both cases, low temperature and/or fast reaction techniques are usually required to observe and study the diiron(III) peroxo complexes due to their intrinsic instability. Only a few such species are relatively stable at room temperature,[23,32] including oxyhemerythrin, which has a half-life of about 1 day.[9]

Intermediates other than Fe^{III}_2-peroxo species have been detected upon the oxygenation of Fe^{II}_2 complexes. A carboxylato-bridged complex, $[Fe^{II}_2(\mu\text{-}O_2CAr^{Tol})_4(4\text{-}^tBuC_5H_4N)_2]$, with bulky ligands reacts with O_2 at −78 °C to give an equimolar mixture of $Fe^{III}Fe^{IV}$ and $Fe^{II}Fe^{III}$ species, which upon heating converts into a hydroxo-bridged diiron(III) complex.[33] The reaction of O_2 with the $[Fe^{II}_2(\mu\text{-OH})(\mu\text{-}O_2CCR_3)_2(Me_3tacn)_2]^+$ complexes affords transient $Fe^{II}Fe^{III}$ species (presumably via an outer-sphere electron transfer), several of which have been isolated and thoroughly characterized.[34]

One of the most versatile synthetic systems, which can model both structural and functional aspects of the native non-heme diiron proteins, are hydroxo- and oxo-bridged diiron complexes with tris(2-pyridylmethyl)amine (TPA) and its derivatives, e.g., tris(6-methyl-2-pyridylmethyl)amine (6-Me_3-TPA).[35−38] Very recently it has been shown that the diferrous $[Fe^{II}_2(\mu\text{-OH})_2(6\text{-}Me_3\text{-TPA})_2]^{2+}$ complex **1** reacts with O_2 to yield a diferric peroxo complex $[Fe^{III}_2(\mu\text{-O})(\mu\text{-}O_2)(6\text{-}Me_3\text{-TPA})_2]^{2+}$ **2**, which upon the addition of 1 equiv of acid converts into a high-valent $[Fe^{III}Fe^{IV}(\mu\text{-O})_2(6\text{-}Me_3\text{-TPA})_2]^{3+}$ species capable of oxidizing 2,4,6-tri-*tert*-butylphenol to the corresponding phenoxy radical (Figure 1, Scheme 2).[39] In this reaction sequence, synthetic diiron complexes can access each step proposed for the cycle of the native RNR R2 protein (Scheme 1). The peroxo complex **2**, which can also be generated from the oxo-bridged diferric precursor $[Fe^{III}_2(\mu\text{-O})_2(6\text{-}Me_3\text{-TPA})_2]^{2+}$ and H_2O_2,[31] has been comprehensively characterized by mass spectrometry, EXAFS, resonance Raman, Mössbauer, and UV−vis spectroscopy.[31,39]

Here, we present a kinetic and mechanistic study of the formation of the diiron(III) peroxo complex **2** from the diiron-

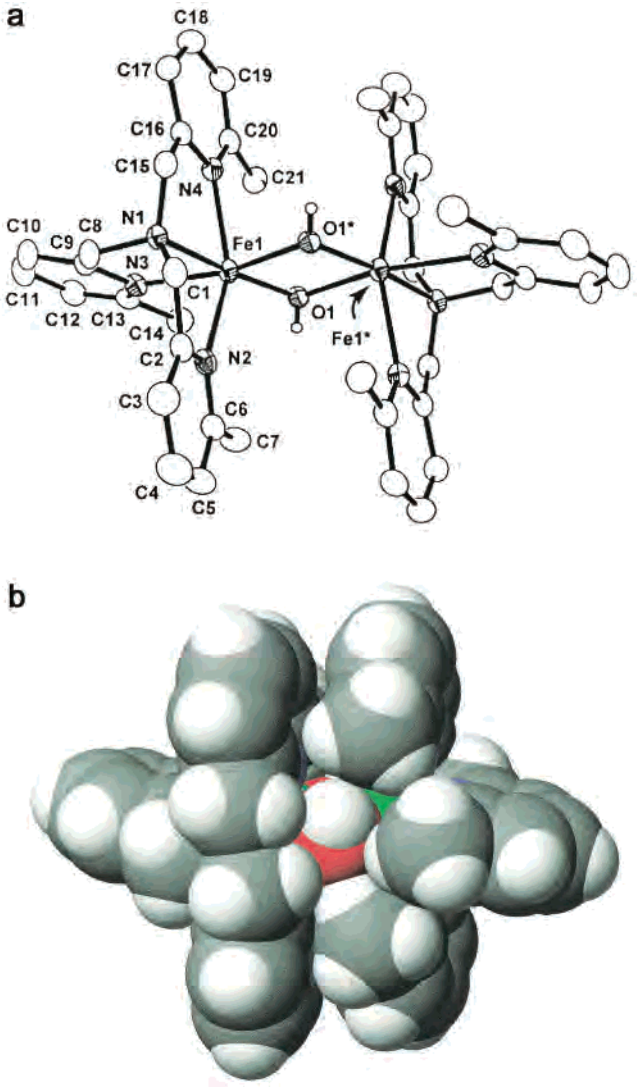

Figure 1. Representations of the crystal structure of $[Fe^{II}_2(\mu\text{-OH})_2(6\text{-}Me_3\text{-TPA})_2]^{2+}$. (a) Ellipsoids drawn at the 50% probability level, and the ligand hydrogen atoms are omitted for clarity (reproduced with permission from ref 39. Copyright 2000 American Chemical Society). (b) Space-filling model generated by the CAChe 3.0 program.

(23) Suzuki, M.; Furutachi, H.; Ôkawa, H. *Coord. Chem. Rev.* **2000**, *200*−*202*, 105−129.
(24) Feig, A. L.; Becker, M.; Schindler, S.; van Eldik, R.; Lippard, S. J. *Inorg. Chem.* **1996**, *35*, 2590−2601.
(25) Feig, A. L.; Masschelein, A.; Bakac, A.; Lippard, S. J. *J. Am. Chem. Soc.* **1997**, *119*, 334−342.
(26) Herold, S.; Lippard, S. J. *J. Am. Chem. Soc.* **1997**, *119*, 145−156.
(27) LeCloux, D. D.; Barrios, A. M.; Mizoguchi, T. J.; Lippard, S. J. *J. Am. Chem. Soc.* **1998**, *120*, 9001−9014.
(28) LeCloux, D. D.; Barrios, A. M.; Lippard, S. J. *Bioorg. Med. Chem.* **1999**, *7*, 763−772.
(29) Than, R.; Schrodt, A.; Westerheide, L.; van Eldik, R.; Krebs, B. *Eur. J. Inorg. Chem.* **1999**, 1537−1543.
(30) Kryatov, S. V.; Rybak-Akimova, E. A. *J. Chem. Soc., Dalton Trans.* **1999**, 3335−3336.
(31) Dong, Y.; Zang, Y.; Shu, L.; Wilkinson, E. C.; Que, L., Jr. *J. Am. Chem. Soc.* **1997**, *119*, 12683−12684.
(32) Hagadorn, J. R.; Que, L., Jr.; Tolman, W. B. *J. Am. Chem. Soc.* **1998**, *120*, 13531−13532.
(33) Lee, D.; Du Bois, J.; Petasis, D.; Hendrich, M. P.; Krebs, C.; Huynh, B. H.; Lippard, S. J. *J. Am. Chem. Soc.* **1999**, *121*, 9893−9894.
(34) Payne, S. C.; Hagen, K. S. *J. Am. Chem. Soc.* **2000**, *122*, 6399−6410.
(35) Que, L., Jr.; Dong, Y. *Acc. Chem. Res.* **1996**, *29*, 190−196.
(36) Que, L., Jr. *J. Chem. Soc., Dalton Trans.* **1997**, 3933−3940.
(37) Hsu, H.-F.; Dong, Y. H.; Shu, L.; Young, V. G., Jr.; Que, L., Jr. *J. Am. Chem. Soc.* **1999**, *121*, 5230−5237.
(38) Zheng, H.; Yoo, S. J.; Münck, E.; Que, L., Jr. *J. Am. Chem. Soc.* **2000**, *122*, 3789−3790.

Scheme 2

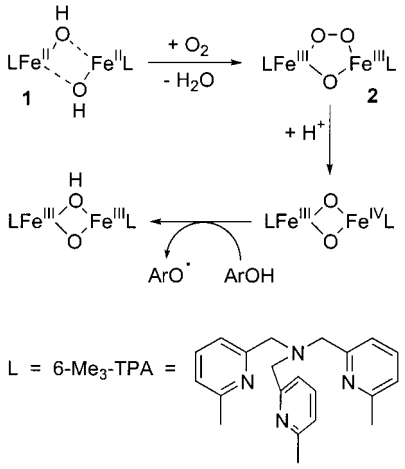

(II) precursor **1** and O_2 (eq 1).

$$[Fe^{II}_2(\mu\text{-OH})_2(6\text{-Me}_3\text{-TPA})_2]^{2+} + O_2 \rightarrow [Fe^{III}_2(\mu\text{-O})(\mu\text{-O}_2)(6\text{-Me}_3\text{-TPA})_2]^{2+} + H_2O \quad (1)$$

Only one similarly detailed kinetic study was performed on a series of three alkoxide-/carboxylate-bridged dinuclear model complexes with five-coordinate iron(II) centers, which exhibited oxygenation reactions at low temperatures leading to peroxo diiron(III) species.[24] The dihydroxy-bridged six-coordinate diiron(II) complex **1** (Figure 1) studied here differs from the previously reported complexes in the nature of bridging ligands and in the coordination saturation of its Fe^{II} centers. We set out to determine how such a change in the coordination of a diiron(II) complex would affect the dynamics of the formation of a diiron(III) peroxo species.

Experimental Section

General Considerations. Complex **1**$(ClO_4)_2$ was prepared as described previously.[39] All manipulations of **1**$(ClO_4)_2$ and its solutions were done inside a Vacuum Atmospheres glovebox with argon or by using Hamilton airtight syringes. Acetonitrile (Aldrich, anhydrous), acetone (Acros, anhydrous), and dichloromethane (Aldrich, anhydrous, stabilized with 50 ppm of amylene) were degassed, transferred into the glovebox, and equilibrated with argon there. Dichloromethane (Fisher, >99.9%, GS/MS grade, not stabilized) was additionally treated with basic aluminum oxide. Oxygen and nitrogen (ultrahigh purity grade, Airgas Northeast) were used as received. Nitric oxide (Airgas Northeast) was passed through a column with moist KOH pellets. Graduated mixtures of oxygen and nitrogen were prepared using Bel-Art gas flow meters. Saturated solutions of O_2, O_2-N_2 mixtures, and NO in solvents were prepared by bubbling the gas through liquid for 20 min in a cylinder closed with a septum and thermostated at 20 or 25 °C. The solubility of O_2 in dichloromethane was accepted to be 5.80 mM at 20 °C;[40,41] in acetone, 11 mM at 25 °C; and in acetonitrile, 8.1 mM at 25 °C.[42] The solubility of NO was assumed to be similar, in the range of 5−10 mM.[43,44]

The low content of water in the commercial anhydrous dichloromethane (<1 mM H_2O) allowed for cryogenic stopped-flow spectrophotometry. No interference with optical measurements at temperatures from −80 to −40 °C was observed. When the lines of the stopped-flow device were washed with dichloromethane, containing 2−3 mM H_2O or more added on purpose (using solvent saturated with water[45]), deposition of a light-absorbing material (presumably a CH_2Cl_2 ice clathrate[46]) was registered at temperatures of −40 °C or below and complicated the measurements.

Temperature Dependence of Dichloromethane Density. A 100 mL glass volumetric flask with a long narrow neck was used. The neck was equipped with a strip of graduated paper, and the flask volume was calibrated with water.[47] A 105 mL sample of dichloromethane was placed into the flask, and its exact mass was determined by weight. The flask was equipped with a tiny stirbar and a thermocouple, their volume was negligible as determined from the level of the liquid meniscus. The volume of the liquid was determined at 5 °C intervals between +25 and −40 °C, both on the drop and the rise of temperature. The data were converted to density and corrected for the contraction of the flask using the average thermal expansion coefficient of glass (2.5×10^{-7} K^{-1}).[47] The data can be very satisfactorily represented by a linear equation (eq 2), which was used to extrapolate the density of dichloromethane at temperatures down to −80 °C. Equation 3 was used to account for the change in reagent concentration in dilute dichloromethane solutions with the change in temperature.

$$d_T = 1.370(2) - 0.00180(2)T \ (T \text{ in } ^\circ\text{C}) \quad (2)$$

$$C_T = C_{20^\circ\text{C}}\,(d_T/d_{20^\circ\text{C}}) \quad (3)$$

Stopped-Flow Kinetic Experiments. Kinetic measurements were performed at temperatures from −80 to −40 °C using a Hi-Tech Scientific (Salisbury, Wiltshire, UK) SF-43 cryogenic stopped-flow instrument equipped with stainless steel plumbing, a 1.00 cm stainless steel mixing cell with sapphire windows, and an anaerobic gas flushing kit. The instrument was connected to an IBM computer with IS-2 Rapid Kinetics software by Hi-Tech Scientific. The mixing cell was maintained to ±0.1 K, and mixing time was 2−3 ms. The anaerobic kit of the apparatus was flushed with nitrogen before and during the experiments. All lines of the SF instrument were extensively washed with oxygen-free, argon-saturated anhydrous solvent before charging the mixing syringes with reactant solutions. In all kinetic experiments, a series of 5−7 shots gave standard deviations within 5%, with overall reproducibility within 10%.

The kinetic data from stopped-flow experiments were treated by two methods. In the integral method, kinetic curves obtained under pseudo-first-order conditions over 2−3 half-lives were fit to eq 4. In the method of initial rates, kinetic data from the first 5−10% of a half-life were fit to a linear function giving dA/dt as the initial rate of absorbance change. Equation 5 was used to convert dA/dt into the bulk pseudo-first-order rate constant k_1, with $\Delta\epsilon = (\epsilon_2 - \epsilon_1)$ being the difference in the molar absorption coefficients of **2** and **1** (per mole of diiron complex).

$$A_t = A_\infty - (A_\infty - A_0)\exp(-k_1 t) \quad (4)$$

$$k_1 = \frac{dA/dt}{\Delta\epsilon[\mathbf{1}]} \quad (5)$$

(39) MacMurdo, V. L.; Zheng, H.; Que, L., Jr. *Inorg. Chem.* **2000**, *39*, 2254−2255.
(40) Battino, R. In *Oxygen and Ozone*; Battino, R., Ed.; Pergamon Press: New York, 1981; Vol. 7.
(41) The Ostwald coefficient L was converted into molar solubility of dioxygen using the following formula: $S = L(P - P_s)/(TR)$, where P is total pressure, P_s is the saturation vapor pressure of solvent, R is the gas constant, and T is temperature. This formula accounts for the fact that the gas bubbled through liquid is being saturated and diluted with the vapor of the liquid.
(42) Achord, J. M.; Hussey, C. L. *Anal. Chem.* **1980**, *52*, 601−602.
(43) Ivanisevic, A.; Reynolds, M. F.; Burstyn, J. N.; Ellis, A. B. *J. Am. Chem. Soc.* **2000**, *122*, 3731−3738.
(44) Lee, K. Y.; Kuchynka, D. J.; Kochi, J. K. *Inorg. Chem.* **1990**, *29*, 4196−4204.
(45) Stephenson, R. M. *J. Chem. Eng. Data* **1992**, *37*, 80−95.
(46) Kaloustian, J.; Rosso, J. C.; Caranoni, C.; Carbonnel, L. *Rev. Chim. Miner.* **1976**, *13*, 334−342.
(47) Lur'e, Y. Y. *Spravochnik po analiticheskoi khimii*; Khimia: Moscow, 1979.

The values of k_1 obtained by both methods agreed within 10% for the experiments carried out in dichloromethane at temperatures from −80 to −40 °C, which suggested that stopped-flow techniques could be used under our experimental conditions for the time spans of 2−3 half-lives in the reaction between **1** and O_2. In another series of experiments, the stopped-flow feeding line with the light absorbing solution of **1** was closed, and a shot was made using only the colorless solution of O_2. The optical absorbance in the cell remained unchanged for at least 20 min at −40 °C and for up to 1 h at −80 °C, proving that the diffusion from feeding lines was negligible during this time.

Results

Experiments in Dichloromethane. Starting solutions of complex **1** and dioxygen in dichloromethane were prepared at 20 °C, and the reaction between them was studied at temperatures from −80 to −40 °C. We found that the solvent contracts significantly on cooling (e.g., by 8% from 20 to −40 °C), which can be accounted for by eq 2. It is interesting to note that the temperature contraction coefficient of CH_2Cl_2 (1.3×10^{-4} K^{-1}) is nearly the same as those reported for $CHCl_3$ (1.2×10^{-4} K^{-1})[25] and EtCN (1.25×10^{-4} K^{-1}).[48]

Commercial dichloromethane usually contains ca. 50 ppm of "amylene" (a mixture of isomeric pentenes), which is added as an inhibitor of autoxidation. Uninhibited CH_2Cl_2 should be purified from the highly reactive products of autoxidation (HCl and $COCl_2$) and kept under an oxygen-free atmosphere. In separate experiments, no difference in the course and the rate of the reaction between **1** and O_2 was found in inhibited and uninhibited dichloromethane. Thus, it appears that complex **2** does not have pronounced reactivity with electron-rich alkenes, a behavior similar to that of other μ-1,2-peroxo diiron(III) complexes.[28]

Mixing the dichloromethane solutions of **1** and O_2 under conditions of excess dioxygen at low temperatures (from −80 to −40 °C) leads to simple first-order kinetic traces as monitored by spectrophotometry (Figure 2). The reaction is quite slow, with a half-life of 5.5 min at −40 °C under the highest available concentration of oxygen (3.14 mM). The observed pseudo-first-order rate constants, determined by both the integral method and by the method of initial rates, are wavelength independent in the region of 400−800 nm (Figure 2). The optical absorbance obtained immediately upon mixing is exactly one-half of the value for the starting solution of **1** in the entire spectral region studied, suggesting that there is no fast chemical process during the mixing "blind" time of our stopped-flow apparatus (2−3 ms). Thus, even if an intermediate is formed in the reaction, its steady-state concentration is too low for unambiguous detection. It should be noted that stopped-flow spectrophotometry allows only for the observation of the intermediates, which are accumulated in a sufficient amount in the course of a reaction and which have an optical spectrum distinct from other species in the reaction sequence.

The final absorbance extrapolated from the kinetic traces allowed for the calculation of the optical spectrum of complex **2** (Figure 3). Parameters of the two bands in the calculated spectrum of **2** in dichloromethane are $\lambda_{max} = 490$ nm ($\epsilon = 1050 \pm 50$ M^{-1} cm^{-1}) and $\lambda_{max} = 640$ nm ($\epsilon = 1100 \pm 50$ M^{-1} cm^{-1}), which are in good agreement with the results of regular spectrophotometry.[39] This result confirms the validity of the stopped-flow technique even for the rather long time spans (up to 20 min at −40 °C and 1 h at −80 °C) under our conditions (see also the Experimental Section).

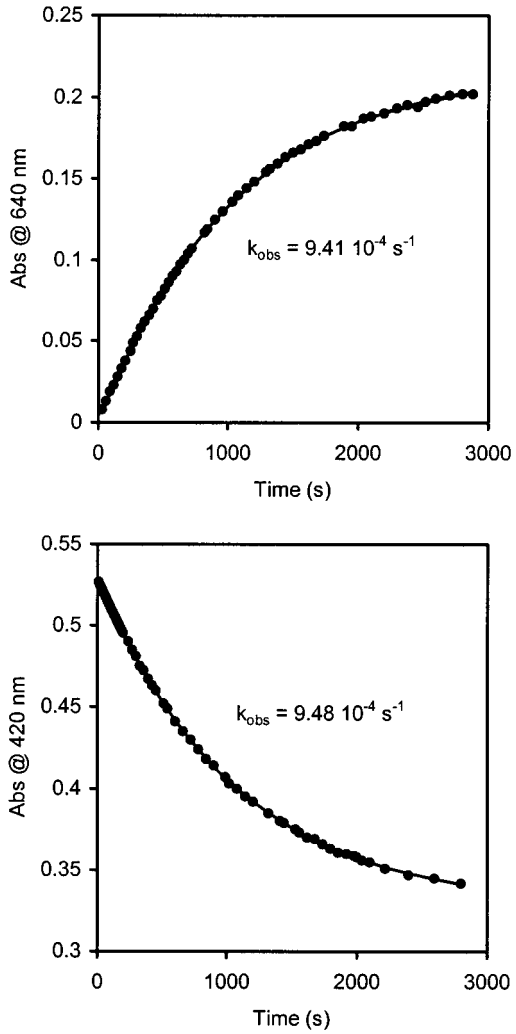

Figure 2. Representative kinetic traces of the reaction between **1** and O_2 in dichloromethane obtained by stopped-flow spectrophotometry. Experimental points superimposed by best single-exponential fit. Conditions: $T = -60$ °C; $[\mathbf{1}]_o = 0.221$ mM and $[O_2]_o = 3.22$ mM.

Thus, oxygenation of the diferrous complex **1** in dichloromethane solution at low temperatures (from −80 to −40 °C) leads to the clean formation of the diferric peroxo species **2** according to eq 1. Above −40 °C the yield of **2** decreases dramatically, suggesting that the peroxo complex is not sufficiently stable at these temperatures. The spectral region near 640 nm is the most convenient region to monitor the reaction, because the starting diferrous complex **1** has a negligible molar absorbance coefficient here, $\epsilon_{640} = 20$ M^{-1} cm^{-1} (Figure 3).

Experimental Rate Law. The dependence of the initial reaction rate on the starting concentration of complex **1**, under excess oxygen at −50 °C, is a straight line with a nearly zero intercept (Figure S1). The overall kinetic curves at different wavelengths, at temperatures from −80 to −40 °C, are fit to a single-exponential eq 4 with mean standard deviations of 2% or less over a period of 2−3 half-lives (Figure 2). No systematic change in the value of the pseudo-first-order rate constant is observed on varying the initial concentration of **1**. Thus, the reaction clearly is first order in the diiron(II) complex **1**.

The solubility of O_2 in dichloromethane is reported to be 5.8 mM at 20 °C.[40,41] Taking into account thermal contraction (eqs 2 and 3) and the 1:1 mixing ratio in the stopped-flow experiments, the maximum accessible concentration of O_2 was ca. 3.2 mM at the temperatures from −80 to −40 °C. Solutions

(48) Karlin, K. D.; Wei, N.; Jung, B.; Kaderli, S.; Niklaus, P.; Zuberbühler, A. D. *J. Am. Chem. Soc.* **1993**, *115*, 9506−9514.

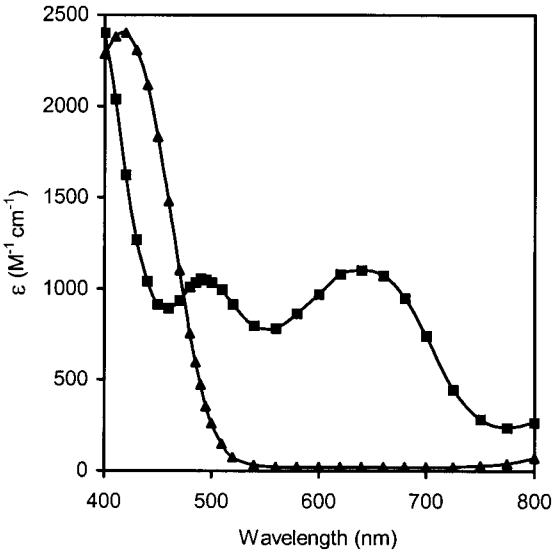

Figure 3. Optical spectra of **1** (triangles) and **2** (squares) in dichloromethane solution obtained in stopped-flow experiments at −60 °C. The spectrum of **2** is calculated from kinetic data (extrapolation on infinite time).

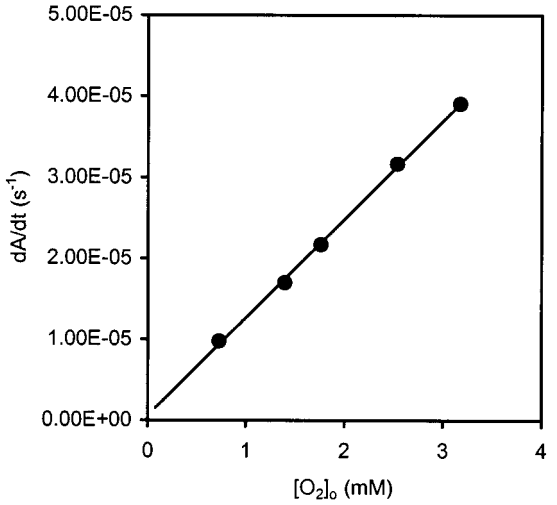

Figure 4. Initial rate of optical absorbance increase at 640 nm vs the starting concentration of O_2 during its reaction with **1** in dichloromethane at −50 °C; $[\mathbf{1}]_o = 0.23$ mM.

with smaller dioxygen concentrations were prepared using calibrated mixtures of O_2 with N_2.

A plot of the initial oxygenation rates, measured at −50 °C, versus the initial concentration of O_2 is a straight line with an almost zero intercept, as displayed in Figure 4. This result shows that the reaction is first order in dioxygen and confirms that it is practically irreversible. Thus, the rate law for the formation of **2** can be described by eq 6. The reaction is second-order overall, its rate constant k_2 being 0.66(6) M^{-1} s^{-1} at −40 °C.

$$d[\mathbf{2}]/dt = -d[\mathbf{1}]/dt = k_2[O_2][\mathbf{1}] = k_1[\mathbf{1}] \qquad (6)$$

Activation Parameters. The rate of oxygenation of **1** in dichloromethane slows down with the decrease in temperature (from −40 to −80 °C) with a van't Hoff's coefficient of only 1.6 ± 0.2 (Table S1). Raw kinetic data were converted into second-order rate constants using eqs 3, 5, and 6 (Tables S1, S2). The Eyring plot of the data obtained by both the method of initial rates and the integral method in the range from −80 to −40 °C is almost linear (Figure 5). Assuming that the reaction

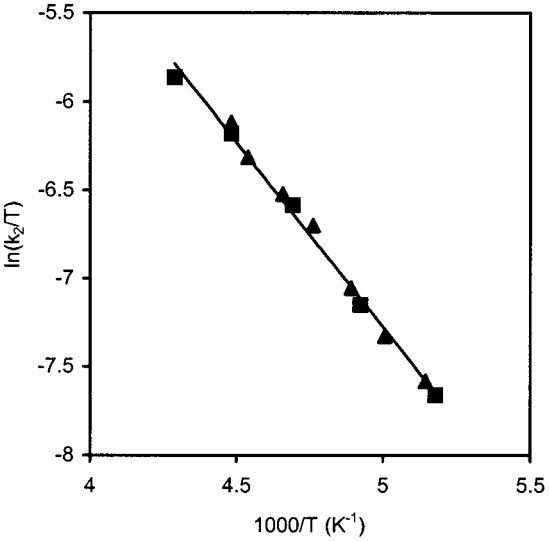

Figure 5. Eyring plot for the reaction of ca. 0.25 mM **1** with ca. 3.2 mM O_2 in dichloromethane based on second-order rate constants calculated from initial rates (triangles) and from integral kinetic data (diamonds).

between **1** and O_2 is a simple bimolecular process, its activation parameters are $\Delta H^{\ddagger} = 17 \pm 2$ kJ mol^{-1} and $\Delta S^{\ddagger} = -171 \pm 20$ J mol^{-1} K^{-1}. Standard states of the reagents are hypothetical 1 M solutions of complex **1** and O_2 in dichloromethane.

Influence of Solvent. Exploratory work was carried out in acetone, acetonitrile, and a dichloromethane−acetonitrile mixture (9:1 by volume) at low temperature (−40 °C and below). The optical spectra of **1** in all solvents are almost identical (λ_{max} = 420 nm, $\epsilon_{max} = 2400$ M^{-1} cm^{-1}), suggesting that the nature of the diferrous reagent does not differ significantly in these solvents. The reaction of **1** with O_2 in the CH_2Cl_2−CH_3CN mixture (9:1) proceeds with approximately the same rate and activation parameters ($\Delta H^{\ddagger} = 17.5 \pm 2$ kJ mol^{-1} and $\Delta S^{\ddagger} = -172 \pm 20$ J mol^{-1} K^{-1}; Figure S2) as it does in neat CH_2Cl_2. The reaction rates in Me_2CO and MeCN are about 1.6 and 5 times faster than in CH_2Cl_2, respectively. However, the formation of **2** from **1** and O_2 in all solvents other than neat dichloromethane is not quantitative (Table S3, Figures S3−S5). For example, in acetonitrile at −40 °C, the maximum absorbance at 650 nm reached at 450 s (ca. 6 half-lives) is only 310 M^{-1} cm^{-1} (Figure S4) versus 1200 M^{-1} cm^{-1} expected for the quantitative formation of **2** in this solvent.[31] Apparently, some byproducts form from **1** and O_2 in the polar solvents, but they were not identified in this work.

Influence of H_2O. The solubility of water in dichloromethane has been reported as 137 mM at 20 °C and 62 mM at 0 °C.[45] Below −0.8 °C, water falls out from this solution as the clathrate, $CH_2Cl_2 \cdot 34H_2O$, and the content of H_2O in the liquid phase drops dramatically.[46]

When water solutions (2−20 mM) in dichloromethane saturated with O_2 are introduced into the stopped-flow lines at low temperatures (−40 °C or below), the accumulation of a light-absorbing material, presumably the clathrate $CH_2Cl_2 \cdot 34H_2O$, is detected. With higher water concentrations no meaningful kinetic or spectrophotometric data can be obtained. With 2−4 mM H_2O the interference is less severe, and the stopped-flow spectrophotometer can be adjusted after every shot. The rate of the reaction between **1** and O_2 in the presence of water is slightly larger (ca. 10%) than it is in anhydrous dichloromethane (Table S3). It should be noted that the process occurs in an evidently nonhomogeneous reaction mixture,

ostensibly consisting of dichloromethane liquid phase saturated with water and a solid icelike phase.

The influence of water on the oxygenation of complex **1** has also been studied in the $CH_2Cl_2-CH_3CN$ mixture (9:1). No apparent formation of a solid phase interfering with optical measurements is observed at −50 °C with water concentrations of up to 20 mM. The initial rate of the reaction between **1** and O_2, measured at 640 nm, is somewhat accelerated by water, by ca. 25% at the maximum [H_2O] used (10 mM after mixing) versus the "dry" solvent mixture (Figure S6). While this acceleration is relatively small and should not be overestimated, the above experiments clearly show that oxygenation of **1** is not retarded by water.

Influence of D_2O. The reaction rate in neat dichloromethane with a small amount of added D_2O (2−4 mM) was slightly larger (5−10%) versus the anhydrous solvent at −40 °C, but the effect could not be measured more accurately due to the deposition of a solid phase at the low temperature. The experiments in the $CH_2Cl_2-CH_3CN$ mixture (9:1) at −50 °C also showed that the effects of H_2O and D_2O on the reaction rate are quite similar (Figure S6).

The hydrogens of the bridging hydroxide ligands in complex **1** should exchange relatively quickly with the solvent water.[49,50] The similar effects of H_2O and D_2O on oxygenation rate suggest that there is no significant isotopic effect upon the H/D substitution in complex **1**.

Influence of Acid. Acid has been shown to accelerate the transformation of the diferric peroxo complex **2** into the high-valent species $[Fe^{III}Fe^{IV}(\mu\text{-}O)_2(6\text{-}Me_3\text{-}TPA)_2]^{3+}$ in acetonitrile at −40 °C.[31] Thus, it would be interesting to determine if acid can interfere with the formation of **2** from **1** and O_2.

Solutions of $HClO_4$ (0.5−2.0 mM) were prepared in the $CH_2Cl_2-CH_3CN$ mixture (9:1), saturated with O_2 at 20 °C, and introduced into the reaction with a 0.5 mM solution of **1** in the same solvent at −50 °C. When ≥ 2 equivs of acid are used, formation of **2** is not observed. Mixing of **1** with excess acid leads to an almost instantaneous spectral change, which is complete within the 2−3 ms "blind" time of our stopped-flow apparatus. No apparent changes occur in the following 30 min. The resulting solution is nearly colorless, with the molar absorbance not exceeding 50 M^{-1} cm^{-1} (per diiron unit) in the range of 400−800 nm. With less than 2 mol of $HClO_4$ per 1 mol of **1**, the reaction is biphasic. The first stage is the almost instantaneous reaction between **1** and acid in a 1:2 ratio, as measured from the decrease in optical absorbance at 420 nm. This stage is complete within the mixing time (2−3 ms). It is followed by a much slower reaction, which is seen as a decrease in absorbance at 420 nm and an increase at 640 nm. The rate constant of this process, measured by the integral method at 640 nm, is nearly the same as that obtained without acid. The initial rates and overall spectral changes correspond to the decreased amount of **1** in the reaction mixture.

Thus, it appears that **1** reacts very quickly with $HClO_4$ to afford new Fe(II) species, most probably the monomeric $[Fe^{II}L(CH_3CN)_n(H_2O)_{2-n}]^{2+}$ complexes. The products are unreactive with O_2 and do not influence the oxygenation of remaining **1**.

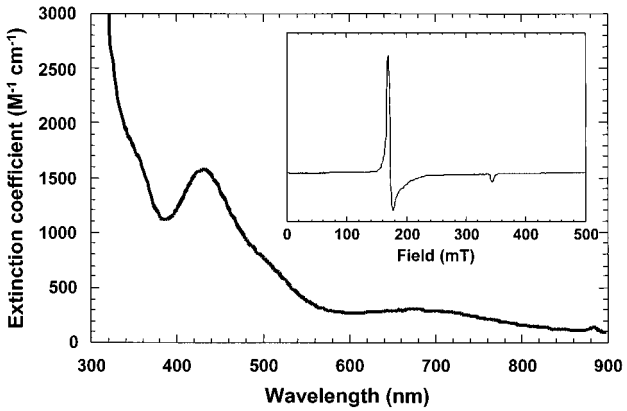

Figure 6. UV-vis spectrum of the reaction product derived from bubbling NO into a 1 mM solution of complex **1** in CH_2Cl_2. Inset: the EPR spectrum of the same reaction mixture. EPR instrumental conditions: microwave power, 0.02 mW; microwave frequency, 9.26 GHz; modulation frequency, 100 kHz; modulation amplitude, 1 mT; and temperature, 4.0 K.

Reaction with NO. Nitric oxide has been used extensively as a probe for oxygen binding iron proteins[51−55] and their synthetic models.[54−58] Reactions with NO and O_2 correlate in their rates for a series of ferrous aminopolycarboxylates, with the rates of nitrosylation being about 3 orders of magnitude faster.[59] Thus, it would be interesting to determine if complex **1** can react with NO and what the rate of the reaction is compared to the rate of oxygenation.

Bubbling NO gas through the dichloromethane solution of **1** at room temperature causes an instant color change from lemon yellow to brown yellow. The UV−vis spectrum of the resulting solution (Figure 6) features maxima at 428 nm (ϵ = 1500 M^{-1} cm^{-1}) and 690 nm (ϵ = 320 M^{-1} cm^{-1}) and a shoulder at 500 nm (ϵ = 900 M^{-1} cm^{-1}). Its EPR spectrum shows signals at g = 4.06, 3.97, and 2.00 (Figure 6), consistent with the formation of an S = 3/2 species. These spectroscopic properties are similar to those reported for $[Fe(6\text{-}Me_3\text{-}TPA)(NO)(O_2CCOPh)]^+$, (388 (sh, ϵ 1200), 492 (ϵ 720), and 690 nm (ϵ 240 M^{-1} cm^{-1}); g = 4.02, 3.93, 1.95),[57] so it is proposed that **1** is converted to $[Fe(6\text{-}Me_3\text{-}TPA)(NO)(OH)]^+$. Very similar visible spectral changes are observed upon mixing the solutions of **1** and NO in stopped-flow experiments at temperatures from −55 to −10 °C in excess nitric oxide (Figure 7). The reaction is much faster than the analogous reaction with dioxygen, the ratio of pseudo-first-order reactions being 1.0×10^3 at −45 °C, under otherwise identical conditions. The apparent activation parameters are $\Delta H^{\ddagger}$ = 29 ± 2 kJ mol^{-1} and $\Delta S^{\ddagger}$ = −77 ± 15 J mol^{-1} K^{-1} (Figure S7).

A Summary of Experimental Results. The diiron(II) complex **1** (0.125−1.0 mM) reacts with dioxygen (1−6 mM)

(49) Relatively slow protonation of bridging oxo ligands in some dinuclear Mn^{III}_2 and Mn^{IV}_2 complexes is known, proceeding with rate constants of about 10^3 M^{-1} s^{-1} at −20 °C.[50] Hydrogen exchange involving the bridging hydroxo ligands in the high-spin Fe^{II}_2 complex **1** should be much faster, because of the significantly smaller degree of π character of the $Fe^{II}-O(H)$ bonds vs the $Mn^{III}-O$ or $Mn^{IV}-O$ bonds.

(50) Carroll, J. M.; Norton, J. R. *J. Am. Chem. Soc.* **1992**, *114*, 8744−8745.

(51) Coufal, D. E.; Tavares, P.; Pereira, A. S.; Hyunh, B. H.; Lippard, S. J. *Biochemistry* **1999**, *38*, 4504−4513.

(52) Haskin, C. J.; Ravi, N.; Lynch, J. B.; Münck, E.; Que, L., Jr. *Biochemistry* **1995**, *34*, 11090−11098.

(53) Carlson, M. L.; Regan, R.; Elber, R.; Li, H.; Phillips, G. N., Jr.; Olson, J. S.; Gibson, Q. H. *Biochemistry* **1994**, *33*, 10597−10606.

(54) Richter-Addo, G. B.; Legzdins, P. *Metal Nitrosyls*; Oxford University Press: New York, 1992.

(55) Hoshino, M.; Laverman, L.; Ford, P. C. *Coord. Chem. Rev.* **1999**, *187*, 75−102.

(56) Zang, Y.; Que, L., Jr. *Inorg. Chem.* **1995**, *34*, 1030−1035.

(57) Chiou, Y.-M.; Que, L., Jr. *Inorg. Chem.* **1995**, *34*, 3270−3278.

(58) Feig, A. L.; Bautista, M. T.; Lippard, S. J. *Inorg. Chem.* **1996**, *35*, 6892−6898.

(59) (a) van Eldik, R. *Abstracts of the 34th Conference on Coordination Chemistry*; Edinburgh, Scotland, 9−14 July 2000. (b) Schneppensieper, T.; Finkler, S.; Czap, A.; van Eldik, R.; Heus, M.; Nieuwenhuizen, P.; Wreesmann, C.; Abma, W. *Eur. J. Inorg. Chem.* **2001**, 491−501.

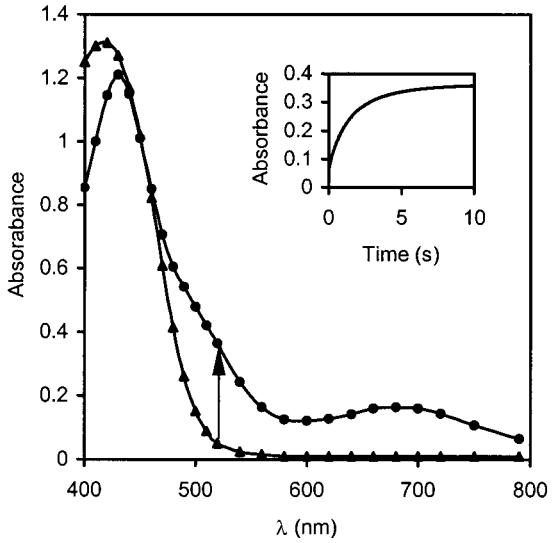

Figure 7. Optical spectra of **1** before (triangles) and after the reaction with NO (squares) obtained by cryogenic stopped-flow technique. Conditions: solution in CH_2Cl_2; $T = -45$ °C; $[\mathbf{1}]_o = 0.55$ mM; $[NO]_o \approx 2.5-5$ mM. Inset: a kinetic trace of the reaction between **1** and NO measured at 520 nm.

in dichloromethane solution at temperatures from −80 to −40 °C to form the diiron(III) peroxo complex **2** almost quantitatively. The reaction is first order in both reagents. No detectable intermediates accumulate in the reaction mixture under the conditions used. The apparent activation parameters of the process are $\Delta H^{\ddagger} = 17 \pm 2$ J mol^{-1} and $\Delta S^{\ddagger} = -175 \pm 20$ J mol^{-1} K^{-1}. The small amount of pentenes (ca. 1 mM) that is present in dichloromethane to stabilize the solvent does not influence the reaction. The oxygenation of **1** in acetone, acetonitrile, and an acetonitrile−dichloromethane mixture proceeds with similar or faster rates, but is not a clean process; the yields of **2** are only 25−60%, with unidentified byproducts also being formed. Addition of water slightly accelerates the rate of the reaction in neat CH_2Cl_2 and in the CH_2Cl_2−CH_3CN mixture. There is no substantial isotopic effect on oxygenation rate upon the H/D exchange in the Fe^{II}−O(H,D)−Fe^{II} bridges of complex **1**. Addition of strong acid in situ destroys the hydroxo complex **1** in a very fast process, converting it into unreactive Fe^{II} species. The diiron(II) complex **1** reacts with NO about 10^3 times faster than with O_2.

Discussion

1. Mechanistic Considerations. The reaction between $[Fe^{II}_2(\mu\text{-OH})_2(6\text{-Me}_3\text{-TPA})_2]^{2+}$ (**1**) and O_2 to form $[Fe^{III}_2(\mu\text{-O})(\mu\text{-O}_2)(6\text{-Me}_3\text{-TPA})_2]^{2+}$ (**2**) is accompanied by the coordination of the dioxygen molecule (involving the formation of two $Fe-O_{peroxo}$ bonds in the eventual μ-1,2 mode), the transfer of two electrons, and the conversion of two μ-OH ligands into one μ-O ligand and a water molecule (involving a proton transfer and breaking of two $Fe-O_{(OH)}$ bonds). The results of kinetic experiments described above help us to understand the sequence of events and to determine the rate-limiting step of the overall process.

1a. Formal Mechanism. The clear first order dependence of the reaction rate with respect to both **1** and O_2 indicates that their association occurs during or before the rate-limiting step. Water dissociates after the rate-limiting step, since the presence of additional water does not retard the reaction. Thus, we can postulate the existence of an intermediate (**1a**), which is an adduct of **1** and O_2 in composition. This intermediate does not accumulate to any appreciable extent as indicated by kinetic spectrophotometric measurements.

Scheme 3

(a) **1** + O_2 $\xrightarrow{\text{slow}}$ **1a** $\xrightarrow{\text{fast}}$ **2**

(b) **1** + O_2 $\underset{K}{\overset{\text{fast}}{\rightleftharpoons}}$ **1a** $\xrightarrow[k]{\text{slow}}$ **1b** $\xrightarrow{\text{fast}}$ **2**

The formation of **1a** in a bimolecular reaction between **1** and O_2 can be the first and rate-limiting step, followed by the fast conversion of **1a** to complex **2** (Scheme 3a). An alternative possibility, indistinguishable from a formal kinetics viewpoint, is that intermediate **1a** forms in a reversible pre-equilibrium in a small, spectroscopically undetectable amount, and converts into another intermediate **1b** in a slow (rate-limiting) step, which is followed by fast events, leading finally to complex **2** (Scheme 3b). The rate of the overall reaction for this case is expressed by eq 7.

$$\frac{d[\mathbf{2}]}{dt} = -\frac{d[\mathbf{1}]}{dt} = \frac{kK[\mathbf{1}][O_2]}{1 + K[O_2]} \qquad (7)$$

If $K[O_2] \ll 1$, eq 7 turns into a second-rate order kinetic equation with a composite rate constant $k_2(\text{obs}) \approx kK$. Analysis of the experimental kinetic data shows that the pre-equilibrium constant K (Scheme 3b) would be quite small ($\ll 10^2$ M^{-1} at −50 °C).[60] Since very low oxygen affinity is uncommon (although not completely unprecedented) for Fe(II) complexes,[23,61] mechanism 3b is not considered to be a likely oxygenation pathway. The associative rate-determining step (Scheme 3a) appears to agree somewhat better with our experimental data. In particular, the activation parameters for the oxygenation of **1** are very similar to those for several other known diiron(II) complexes (vide infra), suggesting a common mechanism. A large negative activation entropy is typical of an associative rate-limiting step.

1b. Molecular Interpretation of the Mechanism. Complex **1** has both Fe^{II} centers six-coordinated (Figure 1). The $Fe^{II}_2(\mu\text{-OH})_2$ diamond core is asymmetric, with a pair of strong (1.973 Å) and a pair of weak (2.168 Å) Fe^{II}−OH bonds.[39] Thus, the dissociation of a weak Fe−OH bond and the formation of a five-coordinate Fe^{II} center could precede the reaction with a new ligand, but it cannot be rate limiting, as indicated by kinetic evidence: 1) the first order of the reaction rate with respect to $[O_2]$, 2) a highly negative value of $\Delta S^{\ddagger}$ (−175 J mol^{-1} K^{-1}) and a small value of $\Delta H^{\ddagger}$ (17 kJ mol^{-1}), and 3) the strong sensitivity of the reaction rate to the nature of the incoming ligand (the reaction with NO is about 10^3 times faster than that with O_2). These data strongly suggest an associative rate-limiting step for the reaction. The direct attack of an O_2 molecule on an Fe^{II} center in complex **1** during or before the rate-limiting step can account for the observations.

The coordination of the O_2 molecule should be accompanied by the simultaneous electron transfer from one or both Fe^{II} centers.[21] A polar transition state is also suggested by the acceleration of the reaction between **1** and O_2 in more polar solvents. The five-fold increase in the oxygenation rate in neat acetonitrile, as compared to neat dichloromethane, cannot be attributed to the coordination of CH_3CN to one or both iron centers, because no acceleration was observed in a CH_2Cl_2−CH_3CN mixture (9:1), in which the coordination of acetonitrile is expected to be almost as likely as in neat CH_3CN.

(60) Taking into account that concentrations of up to 3×10^{-3} M O_2 were used without any detectable (within 10%) deviation from the first order in $[O_2]$ (see Figure 3).

(61) Momenteau, M.; Reed, C. A. *Chem. Rev.* **1994**, *94*, 659−698.

Scheme 4. Possible Alternative Pathways for the Oxygenation of Complex 1

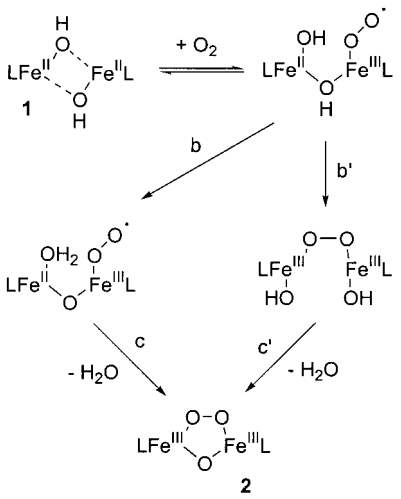

Based on the highly negative value of $\Delta S^{\ddagger}$, it is tempting to propose a concerted mechanism for the O_2 addition, leading directly to a diiron(III) μ-1,2-peroxo complex. However, the two Fe^{II} ions in the starting complex **1** are not sterically accessible for such an attack because of the shielding by two bulky 6-Me_3-TPA ligands (Figure 1). More probable is a stepwise mechanism involving terminal monodentate coordination of the O_2 molecule to one of the iron centers, forming a η^1-superoxo $Fe^{II}Fe^{III}$ complex. In this case, the highly unfavorable activation entropy can be assigned to the steric hindrance at the six-coordinate Fe^{II} ion in complex **1**.

A purely associative (A) mechanism for the O_2 addition would require a seven-coordinated Fe^{III} center in the adduct. Although seven-coordinate ferric complexes are well-known, including a recently characterized Fe^{III} alkylperoxo species,[62] the presence of the bulky 6-Me_3-TPA ligands around the $Fe_2(\mu\text{-}OH)_2$ core in complex **1** creates substantial steric hindrance about the coordination sites (Figure 1) and may be expected to inhibit coordination of a seventh ligand. Breaking of a long weak Fe−OH bond in the asymmetric $Fe_2(\mu\text{-}OH)_2$ core will probably accompany the entrance of the O_2 ligand. Such a mechanism (I_a) is common for 3d transition metal complexes, including Fe^{II} and Fe^{III}.[63]

The η^1-superoxo-μ-hydroxo $Fe^{II}Fe^{III}$ complex is a likely candidate for the putative intermediate **1a** proposed in the formal mechanisms (Scheme 3). Formation of this intermediate from the dinuclear bishydroxo bridged complex **1** and dioxygen involves breaking an Fe−μ-OH bond and forming one Fe−$O_{(O2)}$ bond (accompanied by a formal electron transfer, since dioxygen adducts are usually best formulated as Fe^{III}-superoxo species)[61] (Scheme 4). The value of the activation enthalpy (17 kJ mol^{-1}) is nearly the same as that observed for other reactions in which the association of O_2 and an Fe^{II} center to form an Fe^{III}-superoxo adduct is believed to be the rate-limiting step, including the oxygenation of myoglobin ($\Delta H^{\ddagger} = 21$ kJ mol^{-1}) and monomeric hemoglobin ($\Delta H^{\ddagger} = 24$ kJ mol^{-1}).[10] The highly unfavorable activation entropy can be assigned to the steric hindrance at the six-coordinate Fe^{II} ion in complex **1**, as argued above.

Intermediate **1a** must undergo a second electron transfer, a proton transfer, and the elimination of a water molecule to eventually give complex **2**. The transformation of **1a** into **2** involves the formation of a second Fe−$O_{(O2)}$ bond between the other iron center and the coordinated dioxygen and breaking of another Fe−OH bond. Two possible alternative pathways (b, c or b′, c′) are shown in Scheme 4. The substitution of the terminal hydroxide (pathway b, c) should be more favorable than the substitution of a bridging hydroxide (path b′, c′), especially taking into account the relatively high acidity of a μ-OH ligand, which would facilitate an intramolecular proton transfer (step b) followed by the easy elimination of coordinated water (step c). Experimental findings suggest that water elimination is fast and cannot be involved in a rate-determining step, because the overall reaction is not retarded by water. The proton transfer also cannot be a part of the rate-limiting step, as follows from the absence of a detectable isotopic effect in the experiments with H_2O and D_2O.

The activation parameters of the reaction with NO ($\Delta H^{\ddagger} =$ 29 kJ mol^{-1} and $\Delta S^{\ddagger} = -77$ J mol^{-1} K^{-1}) suggest that both the nitrosylation and oxidation of complex **1** may share a similar associative mechanism with a somewhat later transition state in the former case, leading to a partial compensation effect between $\Delta H^{\ddagger}$ and $\Delta S^{\ddagger}$.

2. Comparison with Other O_2 Binding Metal Complexes. A very limited number of reactions between a diiron(II) precursor and dioxygen to form a peroxo diiron(III) complex have been studied in detail by kinetic techniques and characterized by activation parameters: the oxygenation of myohemerythrin from *Themiste zostericola*,[7,11] soluble methane monooxygenase from *Methylococcus capsulatus*,[13] stearoyl-ACP Δ^9-desaturase from *Ricinus communis*,[14] and three model complexes[24] (Table 1). All of these reactions are irreversible, except for the oxygenation of hemerythrin (Hr). Hr is similar to complex **1** in that it has a hydroxo-bridge between the two Fe^{II} ions in its reduced form. Upon oxygenation, the μ-OH ligand in Hr donates its proton to the nascent peroxo group, giving a μ-O and an η_1-O_2H ligand connected by a hydrogen bond.[1] Complex **1** has a second μ-OH ligand, which can condense with a η_1-O_2H ligand to form a μ-O_2 ligand and H_2O. This condensation may account for the observed irreversibility of the overall reaction between **1** and O_2. The existence of an η^1-superoxo $Fe^{II}Fe^{III}$ intermediate has been postulated for Hr[8] and MMO[12] and considered for other diiron enzymes,[21] but so far not observed directly.

The majority of the reactions listed in Table 1, including the oxygenation of **1**, appear to have an associative rate-limiting step, since they are first order in $[O_2]$ and have significantly negative $\Delta S^{\ddagger}$ values (−175 to −46 J mol^{-1} K^{-1}). Two systems in Table 1 differ from this trend. The oxygenation of reduced MMO is zero order in $[O_2]$, has positive $\Delta S^{\ddagger}$, and the largest $\Delta H^{\ddagger}$ (92 kJ mol^{-1}), all of which suggest a dissociative rate-limiting step. This hypothesis is confirmed by the observation that the nitrosylation of the reduced form of MMO is independent of [NO] and proceeds with nearly the same rate as its oxygenation.[51] The oxygenation of a synthetic diiron(II) complex $[Fe_2(HPTMP)(OBz)]^{2+}$ has an intermediate $\Delta H^{\ddagger}$ (42 kJ mol^{-1}), a moderately negative $\Delta S^{\ddagger}$ (−63 J mol^{-1} K^{-1}), and a partial (0.65) order in $[O_2]$, indicating a complex mechanism.[24] With the very limited number of systems investigated thus far, it is still unclear what factors determine whether an oxygenation follows a dissociative or associative pathway.

All reactions in Table 1 with probable associative pathways have similarly small $\Delta H^{\ddagger}$ values (15−22 kJ mol^{-1}); this is apparently characteristic of the coordination of O_2 to an Fe^{II} center. The oxygenation rates of dinuclear iron(II) complexes, which are relatively slow in this case, are limited by the

(62) Wada, A.; Ogo, S.; Watanabe, Y.; Mukai, M.; Kitagawa, T.; Jitsukawa, K.; Masuda, H.; Einaga, H. *Inorg. Chem.* **1999**, *38*, 3592−3593.
(63) Jordan, R. B. *Reaction mechanisms of inorganic and organometallic systems*; Oxford University Press: New York, 1998.

Table 1. Activation Parameters for the Formation of Diiron(III) Peroxide Complexes from Diiron(II) Precursors and O_2

starting Fe^{II}_2 complex	solvent	T, °C	order in $[O_2]$	$\Delta H^{\ddagger}$ (kJ mol^{-1})	$\Delta S^{\ddagger}$ (J mol^{-1} K^{-1})	ref.
1	CH_2Cl_2	−80°−40°C	1	17 ± 2[a]	−175 ± 20[a]	this work
$[Fe_2(HPTP)(OBz)]^{2+}$	EtCN	−70°−20°C	1	16.5 ± 0.4	−114 ± 2	24
$[Fe_2(EtHPTB)(OBz)]^{2+}$	EtCN	−75°−10°C	1	15.4 ± 0.6	−121 ± 3	24
$[Fe_2(HPTMP)(OBz)]^{2+}$	EtCN	−45°+20°C	0.65	42.2 ± 1.6	−63 ± 6	24
Hr	H_2O	+5°+25°C	−	0.6 ± 0.2	−58 ± 2	7
Hr	H_2O	−	1	17[b]	−46[b]	11
MMOH	H_2O	+3°+35°C	0	92 ± 17	88 ± 42	13
Δ9D	H_2O	+6°+24°C	−	22	−134	14

[a] Standard state is 1 M solution in dichloromethane. [b] Calculated from ΔH, ΔS, $\Delta H^{\ddagger}_{off}$, and $\Delta S^{\ddagger}_{off}$.

activation entropy, which may depend on the steric hindrance about the Fe^{II} sites. Indeed, complex **1** has both Fe^{II} ions six-coordinated and the most unfavorable (negative) $\Delta S^{\ddagger}$ (Table 1). All other studied diferrous enzymes and model compounds have at least one Fe^{II} center with an unsaturated coordination sphere (five- or even four-coordinate Fe^{II}).[11,13,14,24] An increase in steric hindrance at the oxygen-binding site, leading to more negative (unfavorable) activation entropy of oxygenation, is well documented for mononuclear iron(II) and cobalt(II) dioxygen carriers.[64] The low barrier associative oxygen binding to the five-coordinate diiron(II) model complexes, studied by Lippard and co-workers,[24] is typical for the oxygenation reaction at a vacant metal site. A small $\Delta H^{\ddagger}$ value for the O_2 binding to the dihydroxy-bridged six-coordinate diiron(II) complex **1** determined in this work is unexpected, since an $Fe^{II}-OH$ bond breaking event is necessary for the formation of the peroxo complex **2**. It is interesting that the rate-limiting step for the six-coordinate diiron(II) complex still involves the $Fe-O_2$ bond formation.

The rates of dioxygen binding to different classes of synthetic model complexes vary substantially.[61,64] Dicopper(I) complexes have been studied the most thoroughly, yielding examples of both very fast and relatively slow oxygenation.[65] Activation enthalpies of these reactions were usually quite low (ranging from nearly zero to +30 kJ mol^{-1}), with unfavorable activation entropies (from −167 to −66 J mol^{-1} K^{-1}) accounting for the cases of slow oxygen binding. An "open super-oxo" $Cu^{I}Cu^{II}$ complex was inferred in some cases as an intermediate with a low steady-state concentration, but was not observed directly. Some mononuclear iron(II) and cobalt(II) models are capable of very efficient low barrier dioxygen binding at a metal center with a vacant coordination site, with the rates comparable to those for hemoglobin and myoglobin.[64,66,67] Reactions involving metal−solvent bond breaking in the rate-limiting step are usually several orders of magnitude slower and are enthalpically controlled.[64,67]

Kinetic parameters for O_2 binding by natural oxygen carriers are remarkably similar,[10] regardless of the nature of the active site (mononuclear iron(II) porphyrin in myoglobin and hemoglobin, dinuclear iron(II) in hemerythrin, or dinuclear copper(I) in hemocyanin). All of them provide pathways for low-barrier oxygenation ($\Delta H^{\ddagger}$ from 17 to 32 kJ/mol) and do not suffer from unfavorable (large negative) activation entropy, having $\Delta S^{\ddagger}$ values in the range from −60 to +20 J mol^{-1} K^{-1}.[10] As a result, O_2 binding to respiratory metalloproteins is very fast at room temperature (k_{on} on the order of 10^7 M^{-1}s^{-1}).[10,64]

Dioxygen binding to oxygen activating nonheme diiron enzymes (MMO, R2 RNR, and stearoyl-ACP Δ^9-desaturase) is about 10^2-10^4 times slower under comparable conditions.[68] The limited amount of available data show that both a relatively high $\Delta H^{\ddagger}$ (92 kJ mol^{-1} for MMO) and unfavorably negative $\Delta S^{\ddagger}$ (−134 kJ mol^{-1} for Δ^9-desaturase) may account for the slower rates. The different kinetic parameters for the two groups of metalloproteins are consistent with their physiological functions (dioxygen transport versus activation).

Conclusions

The reactions between a hydroxo-bridged diiron(II) complex with dioxygen and nitric oxide have been studied by cryogenic stopped-flow spectrophotometry. The reaction with O_2 leads to a peroxo-bridged diiron(III) complex, resembling the first step in the reactivity of several natural nonheme diiron proteins. The mechanistic results suggest an associative rate-limiting step for the oxygenation of the diiron(II) precursor, similar to that of stearoyl-ACP Δ^9-desaturase, but distinct from the probable dissociative pathway of methane monoxygenase. The existence of a steady-state intermediate, most likely an η^1-superoxo Fe^{II}-Fe^{III} complex, is also inferred by the analysis of the experimental data.

Acknowledgment. This work was supported by the National Institutes of Health (grant GM-38767 to L.Q.), by an award from Research Corporation (grant RI 02233 to E.V.R.-A.), and by Tufts University.

Supporting Information Available: Additional kinetic and spectral data (Tables S1-S3; Figures S1-S7). This material is available free of charge via Internet at http://pubs.asc.org.

IC001300K

(64) Warburton, P. R.; Busch, D. H. In *Dynamics of iron(II) and cobalt-(II) dioxygen carriers*; Warburton, P. R.; Busch, D. H., Ed.; JAI Press: London, 1993; Vol. 2, pp 1−79.
(65) Karlin, K. D.; Kaderli, S.; Zuberbühler, A. D. *Acc. Chem. Res.* **1997**, *30*, 139−147.
(66) Rybak-Akimova, E. V.; Otto, W.; Deardorf, P.; Roesner, R.; Busch, D. H. *Inorg. Chem.* **1997**, *36*, 2746−2753.
(67) Rybak-Akimova, E. V.; Marek, K.; Masarwa, M.; Busch, D. H. *Inorg. Chim. Acta* **1998**, *270*, 151−161.

(68) The pseudo-first-order rate constants measured for the oxygenation of the nonheme diiron(II) enzymes at $[O_2] \approx 10^{-3}$ M and $T \approx 5$ °C are within $1-10^2$ s^{-1}.[12−14, 22] The pseudo-first-order rate constants of O_2 binding by the natural oxygen carriers can be estimated as 10^4 s^{-1} under the similar conditions of $[O_2]$ and temperature.[10]